ORIGINAL PAPER

Hai-Shun Wu · Haijun Jiao

Boron nitride cages from $B_{12}N_{12}$ to $B_{36}N_{36}$: square–hexagon alternants vs boron nitride tubes

Abstract The structures and stabilities of square–hexagon alternant boron nitrides (B_xN_x, $x = 12$–36) vs their tube isomers containing octagons, decagons and dodecagons have been computed at the B3LYP density functional level of theory with the correlation-consistent cc-pVDZ basis set of Dunning. It is found that octagonal $B_{20}N_{20}$ and $B_{24}N_{24}$ tube structures are more stable than their square–hexagon alternants by 18.6 and 2.4 kcal mol^{-1}, respectively, while the square–hexagon alternants of other cages are more stable. Trends in stability as a function of cluster size are discussed.

Introduction

Boron nitrides B_xN_x have been studied extensively since they are the isoelectronic analogs of the carbon fullerenes. Boron nitride molecules [1, 2] and nanotubes [3–6] have been synthesized and/or characterized. For small molecules ($x = 3$–10), ring isomers are the most stable form of boron nitride [7, 8]. For $x > 10$, cages consisting of three-coordinate networks of boron and nitrogen are the most stable species [9, 10]. A wide variety of cage

isomers exists, and the various classes of cages have been studied to determine which cages are the most stable. For example, fullerene-like cages with pentagons and hexagons in the cage network have been compared to cages with squares and hexagons containing alternate B–N bonds (alternant cage). Theoretical calculations comparing these two classes of molecules predict that the square–hexagon alternants are more stable than fullerene-like molecules for $x = 12$ [11], $x = 13$, 14 and 16 [12] and $x = 24$ [13]. The energetic penalty associated with the pentagons and their inevitable non-alternate B–B and N–N bonds is the determining factor in the relative stability of these two classes. The most stable cages should have only polygons with an even number of atoms, so that full alternation of the boron and nitrogen atoms can take place, resulting in all the bonds being B–N bonds.

However, even-sided polygons include polygons larger than squares and hexagons, and molecules with octagons and larger even-sided polygons have been studied as well. For $x = 24$, Pokropivny et al. [14] predicted that the most stable spheroidal structure has 12 squares, 8 hexagons and 6 octagons. More recently, a $B_{24}N_{24}$ cage with 8 squares, 16 hexagons and 2 octagons was shown [13] to be the most stable, but only slightly more stable than a square–hexagon alternant (6 squares and 20 hexagons).

An interesting result from the most recent study on $B_{24}N_{24}$ [13] is that the most stable octagon-containing molecule is an octagonal tube with exactly two octagons, more specifically with the octagons at each end of a tube consisting of squares and hexagons. Each such tube has a C_4 axis of symmetry down the center of the molecule. In the current study, a stability comparison is made between these tube structures and alternant cages composed entirely of squares and hexagons. However, such tubes exist only if $x = 4n$, where n is a positive integer. For molecule sizes where $x = 4n + 2$, the tube will be capped on one end by an additional ring of four alternating B and N atoms. Over a range of molecule sizes from $x = 12$ to 36, calculations are carried out to determine how the stability relationship between these two

H.-S. Wu (✉) · X.-Y. Cui · X.-F. Qin
Department of Chemistry, Shanxi Normal University,
Linfen, 041004, China
E-mail: wuhs@dns.sxtu.edu.cn

D. L. Strout
Department of Physical Sciences, Alabama State University,
Montgomery, AL 36101, USA
E-mail: dstrout@alasu.edu

H. Jiao
Leibniz-Institut für Organische Katalyse, Universität Rostock,
Albert-Einstein-Strasse 29a, 18059 Rostock, Germany
E-mail: haijun.jiao@ifok-rostock.de

classes of molecules varies with the size of the molecules. For each molecule size x, if F_4, F_6 and F_8 represent the number of squares, hexagons and octagons, respectively, the molecules are subject to the following mathematical bounds:

$$F_4 - F_8 = 6 \text{ (Euler's theorem)} \tag{1}$$

$$F_4 + F_6 + F_8 = x + 2 \tag{2}$$

The alternant cages have $F_4 = 6$ and $F_8 = 0$, whereas the fully open tube structures have $F_4 = 8$ and $F_8 = 2$. The capped tube structures have $F_4 = 7$ and $F_8 = 1$, the one octagon on the uncapped end. Further, tube structures are chosen such that each octagon is adjacent to four squares that surround it in a fourfold symmetry (capped tubes only have a twofold symmetry overall because of the structure of the cap). Such square–octagon adjacency has been shown [13] to have a stabilizing influence on the molecules. Trends in stability will be discussed over the range of all even x from 12 to 36. The molecule size $x = 14$ is excluded because no square–hexagon isomer exists for $B_{14}N_{14}$ without edge-sharing squares.

Also, the square–hexagon alternants will be compared to decagonal and dodecagonal tube-shaped molecules, at molecule sizes where such tube molecules exist. The decagonal tube has a ten-membered ring and five adjacent squares at each end, and the structure and energy of decagonal tubes will be calculated for $x = 20$ and 30 (sizes at which the number of atoms is a multiple of ten). Likewise, the structure and energy of dodecagonal tubes, which have a 12-membered ring and six adjacent squares at each end, are calculated for $x = 18$, 24, 30 and 36 (sizes at which the number of atoms is a multiple of 12). Trends of stability for decagonal and dodecagonal tubes will be discussed as a function of cluster size.

Computational details

Geometries of all the molecules in this study were optimized with the B3LYP density functional method
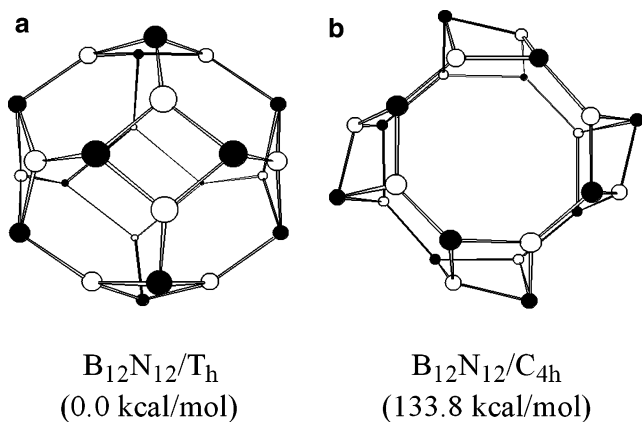
[15, 16]. The basis set [17] was the correlation-consistent double-zeta (cc-pVDZ) set of Dunning. All optimized geometries were characterized as energy- minimum structures by frequency analysis. All calculations were carried out with the Gaussian 98 quantum chemistry software package [18].

B$_{16}$N$_{16}$/T$_d$
(0.0 kcal/mol)

B$_{16}$N$_{16}$/S$_8$
(61.0 kcal/mol)

Fig. 2 $B_{16}N_{16}$ molecules: (a) square–hexagon alternant; (b) octagonal tube

B$_{18}$N$_{18}$/S$_6$
(0.0 kcal/mol)

B$_{18}$N$_{18}$/C$_2$
(8.9 kcal/mol)

B$_{18}$N$_{18}$/C$_{6h}$
(408.4 kcal/mol)

Fig. 3 $B_{18}N_{18}$ molecules: (a) square–hexagon alternant; (b) capped octagonal tube; (c) dodecagonal tube

B$_{12}$N$_{12}$/T$_h$
(0.0 kcal/mol)

B$_{12}$N$_{12}$/C$_{4h}$
(133.8 kcal/mol)

Fig. 1 $B_{12}N_{12}$ molecules: (a) square–hexagon alternant; (b) octagonal tube

Results and discussion

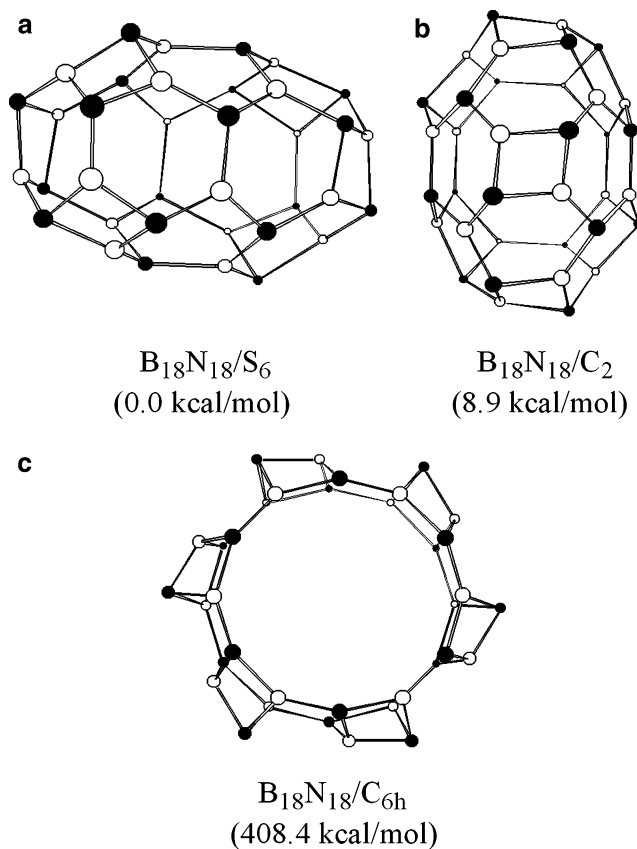Twelve different molecule sizes were considered in this study, and the structures of the molecules are shown in Figs. 1, 2, 3, 4, 5, 6, 7, 8, 9, 10, 11 and 12, respectively, for B_xN_x molecules with $x = 12, 16, 18, 20, 22, 24, 26, 28,$
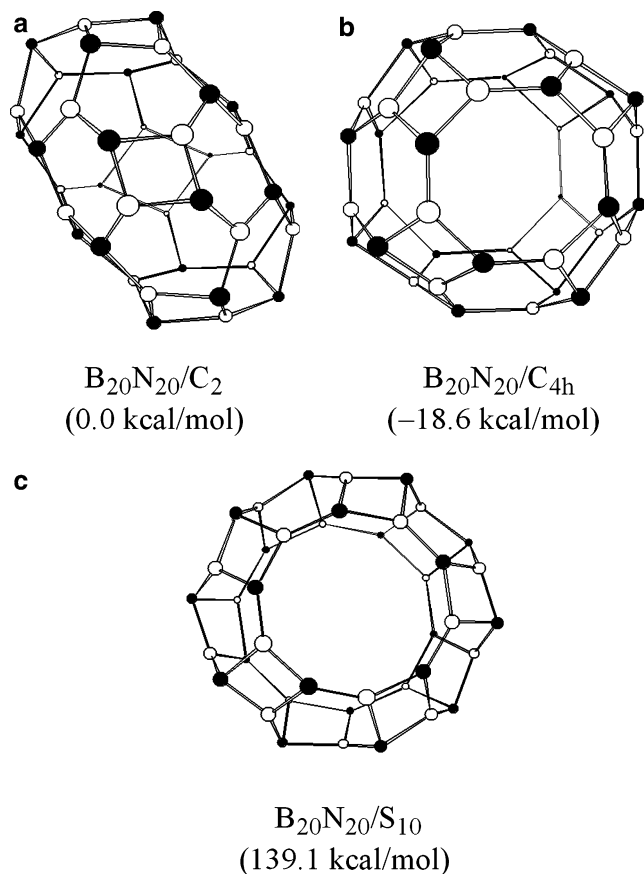

B$_{20}$N$_{20}$/C$_2$
(0.0 kcal/mol)

B$_{20}$N$_{20}$/C$_{4h}$
(−18.6 kcal/mol)

B$_{20}$N$_{20}$/S$_{10}$
(139.1 kcal/mol)

Fig. 4 $B_{20}N_{20}$ molecules: (a) square–hexagon alternant; (b) octagonal tube; (c) decagonal tube

B$_{22}$N$_{22}$/C$_3$
(0.0 kcal/mol)

B$_{22}$N$_{22}$/C$_2$
(16.1 kcal/mol)
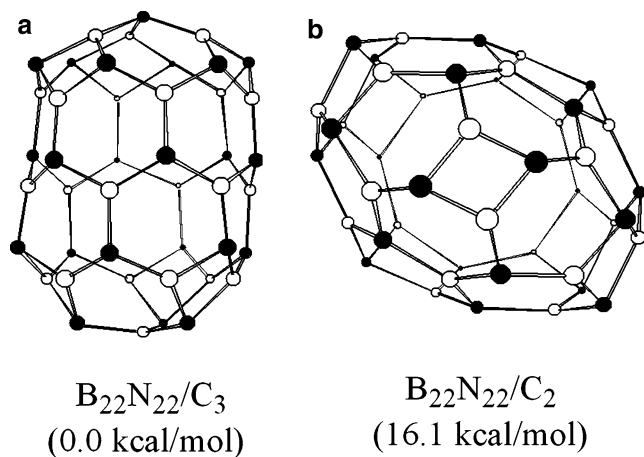
Fig. 5 $B_{22}N_{22}$ molecules: (a) square–hexagon alternant; (b) capped octagonal tube

B$_{24}$N$_{24}$/S$_4$
(0.0 kcal/mol)

B$_{24}$N$_{24}$/S$_8$
(−2.4 kcal/mol)

B$_{24}$N$_{24}$/S$_{12}$
(330.6 kcal/mol)

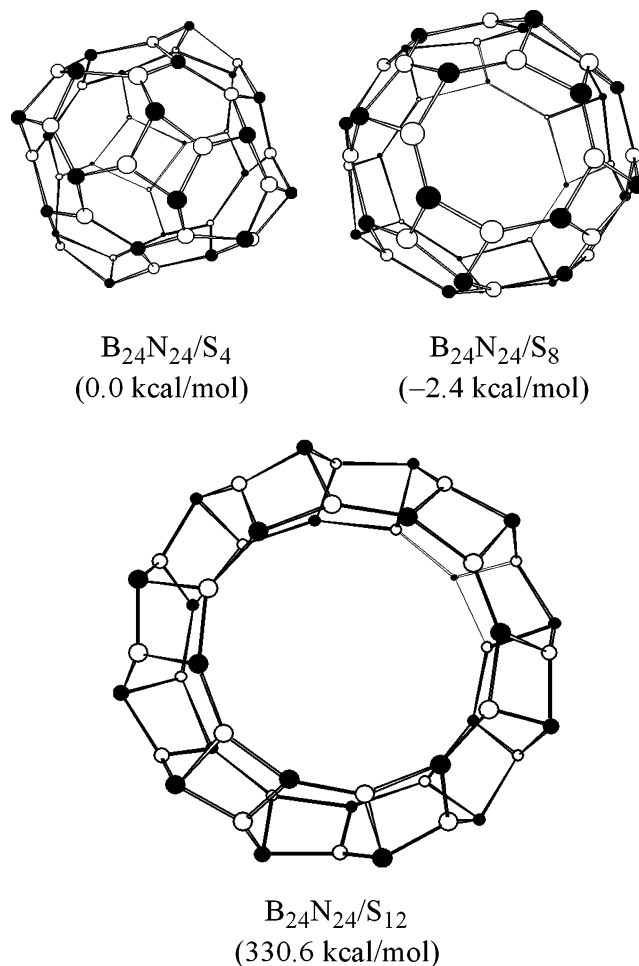**Fig. 6** $B_{24}N_{24}$ molecules: (a) square–hexagon alternant; (b) octagonal tube; (c) dodecagonal tube

B$_{26}$N$_{26}$/C$_{2h}$
(0.0 kcal/mol)

B$_{26}$N$_{26}$/C$_2$
(13.2 kcal/mol)
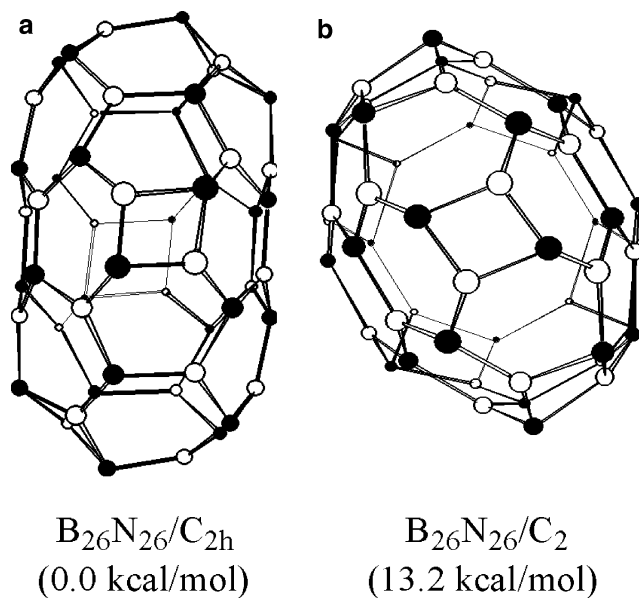
Fig. 7 $B_{26}N_{26}$ molecules: (a) square–hexagon alternant; (b) capped octagonal tube

B$_{28}$N$_{28}$/T
(0.0 kcal/mol)

B$_{28}$N$_{28}$/C$_{4h}$
(28.2 kcal/mol)
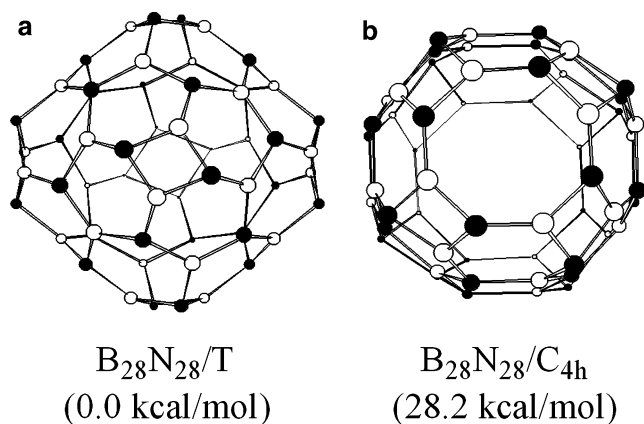
Fig. 8 B$_{28}$N$_{28}$ molecules: (a) square–hexagon alternant; (b) octagonal tube

B$_{32}$N$_{32}$/C$_1$
(0.0 kcal/mol)

B$_{32}$N$_{32}$/S$_8$
(7.7 kcal/mol)

Fig. 10 B$_{32}$N$_{32}$ molecules: (a) square–hexagon alternant; (b) octagonal tube

30, 32, 34 and 36. Total energies for the square–hexagon alternants and tubes are given in Table 1, and their relative energies in Table 2. From the data, the following general trends are evident.

Octagonal tubes

For $x = 12$, the octagonal tube is unstable by 133.8 kcal mol^{-1} above the square–hexagon alternant because the eight squares form four edge-sharing pairs (Fig. 1), which is a destabilizing feature that is inevitable for very short tubes. The separation of squares first occurs for $x = 16$, but the octagonal tube is still 61.0 kcal mol^{-1} less stable than the square–hexagon alternant (Fig. 2). As the tube is lengthened, however, the octagonal tube becomes much more energetically competitive ($x = 18$, Fig. 3), becoming more stable than the alternant at the intermediate sizes ($x = 20, 24$, Figs. 4, 6). Toward the upper end of molecule sizes in this study, the octagonal tubes show signs of becoming less stable, but they are still close in energy to their square–hexagon alternants. It may be the case, however, that the gap widens again for very large sizes. The octagons do not incur a substantial energy penalty in the molecules in this study,

B$_{34}$N$_{34}$/C$_3$
(0.0 kcal/mol)

B$_{34}$N$_{34}$/C$_2$
(49.0 kcal/mol)

Fig. 11 B$_{34}$N$_{34}$ molecules: (a) square–hexagon alternant; (b) capped octagonal tube

and octagon-containing molecules are close in energy to alternants over a range of sizes.

Capped octagonal tubes

Capping one end of the octagonal tube with a square (to produce molecules with $x = 4n + 2$ as opposed to $4n$) also does not incur an energetic penalty for the molecules. Capped tubes, with a single octagon, are very close in energy to the square–hexagon alternants over a wide

B$_{30}$N$_{30}$/C$_2$
(0.0 kcal/mol)

B$_{30}$N$_{30}$/C$_2$
(21.3 kcal/mol)

B$_{30}$N$_{30}$/S$_{10}$
(54.0 kcal/mol)

B$_{30}$N$_{30}$/C$_{6h}$
(226.0 kcal/mol)

Fig. 9 B$_{30}$N$_{30}$ molecules: (a) square–hexagon alternant; (b) capped octagonal tube; (c) decagonal tube; (d) dodecagonal tube

Fig. 12 $B_{36}N_{36}$ molecules: (a) square–hexagon alternant; (b) octagonal tube; (c) dodecagonal tube

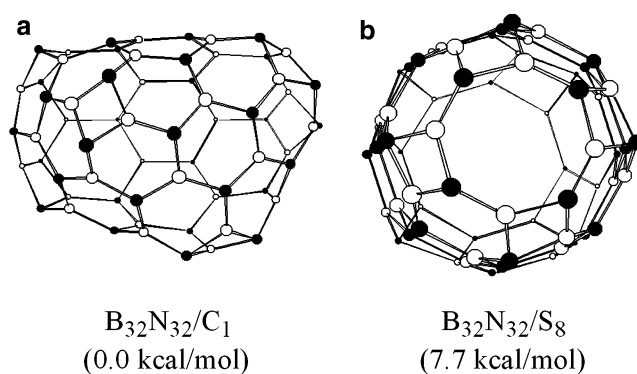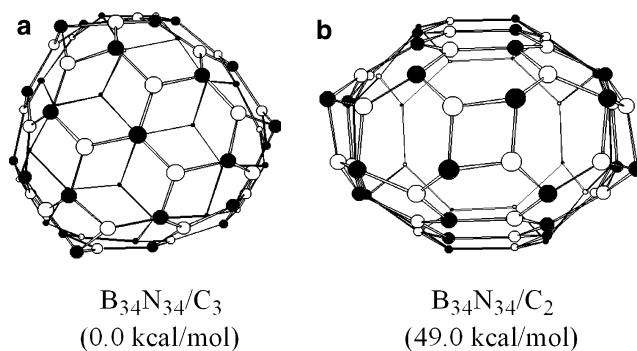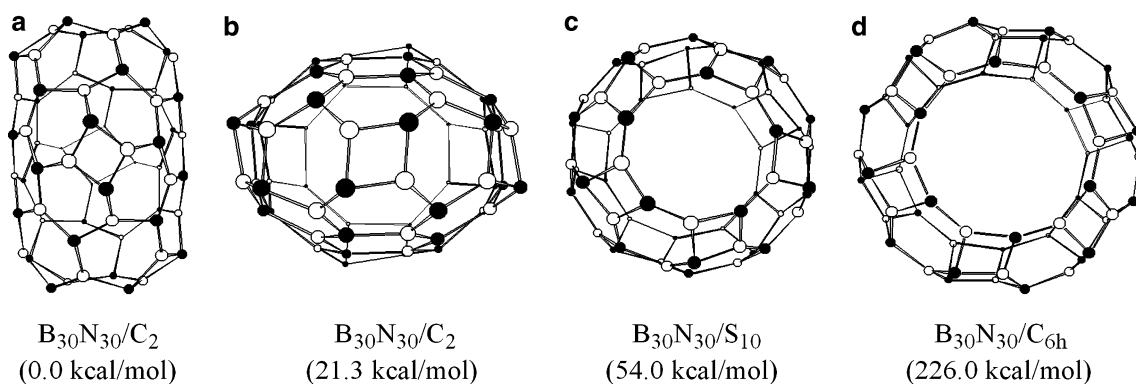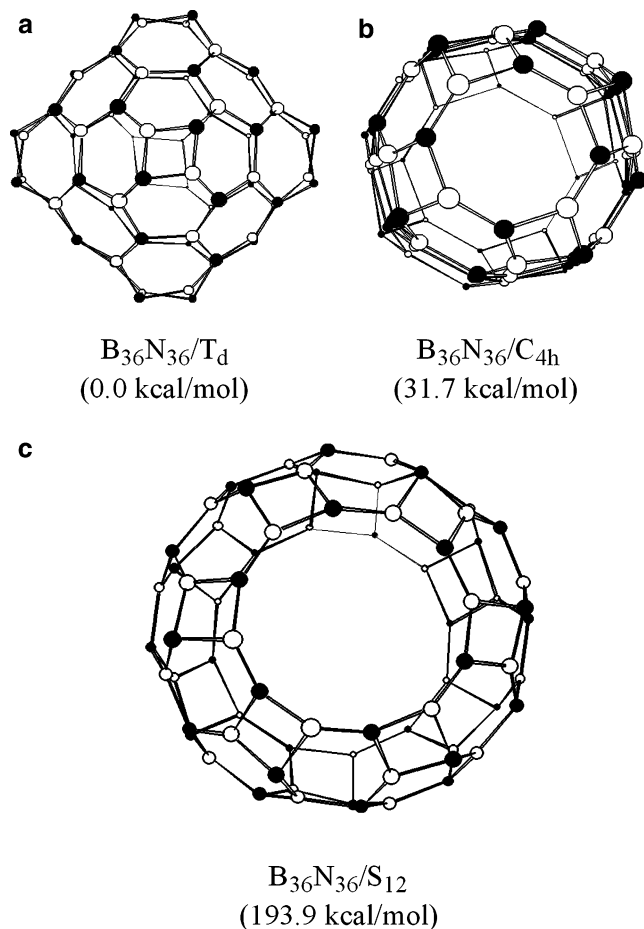square–hexagon alternant structure (Fig. 8) is the most stable isomer, and structures with one or more octagons are higher in energy among ten isomers containing squares, hexagons and octagons [19]. For $B_{32}N_{32}$, the square–hexagon alternant structure (Fig. 10) is the most stable isomer, and other isomers are higher in energy [20].

Decagonal and dodecagonal tubes

The decagonal tubes for $x = 20$ and 30 show much more favorable stability for the longer $x = 30$ tube relative to the respective square–hexagon alternants as these molecule sizes. However, the $x = 30$ decagonal tube is still over 50 kcal mol^{-1} higher in energy than the corresponding square–hexagon alternant, so that studies of $x = 40$ and 50 would probably be required to establish whether these tubes become energetically competitive with molecules composed entirely of squares and hexagons. The dodecagonal tubes also show a trend of increasing stability with increasing length, and are very much higher in energy at all molecule sizes relative to the square–hexagon alternants. Even for $x = 30$ and 36, these tubes are about 200 kcal mol^{-1} above the square–hexagon molecules, with no sign of significant stabilization. The dodecagonal tubes would likely remain high in energy even at sizes larger than the range studied here.

Conclusion

Boron nitride cages are the most stable if all the polygons have an even number of atoms, but even within that framework, several types of molecules exist with comparable stability, as found previously. Squares and hexagons are not the only structural features that lead to stable molecules. A systematic investigation of square–hexagon alternants and tubes of various diameters reveals that octagonal tubes are comparable in stability

range. For $x = 18$, 22, 26 and 30, the capped octagonal tubes are within 9–22 kcal mol^{-1} of the square–hexagon alternants. The capped octagonal tube is not as stable for $x = 34$, which may be a special case since the smaller sizes do not show a strong trend upward in energy for the capped octagonal tubes. For $B_{28}N_{28}$, the

Table 1 B3LYP/cc-pvDZ total energies (E_{tot}, au) for B_xN_x ($x = 12$–36)

B_xN_x	Symmetry	E_{tot}	B_xN_x	Symmetry	E_{tot}
$B_{12}N_{12}$ (1a)	T_h	−956.18558	$B_{26}N_{26}$ (7a)	C_{2h}	−2072.26843
$B_{12}N_{12}$ (1b)	C_{4h}	−955.97237	$B_{26}N_{26}$ (7b)	C_2	−2072.24745
$B_{16}N_{16}$ (2a)	T_d	−1275.08805	$B_{28}N_{28}$ (8a)	T	−2231.77243
$B_{16}N_{16}$ (2b)	S_8	−1274.99081	$B_{28}N_{28}$ (8b)	C_{4h}	−2231.72748
$B_{18}N_{18}$ (3a)	S_6	−1434.47716	$B_{30}N_{30}$ (9a)	C_2	−2391.17447
$B_{18}N_{18}$ (3b)	C_2	−1434.46296	$B_{30}N_{30}$ (9b)	C_2	−2391.14047
$B_{18}N_{18}$ (3c)	C_{6h}	−1433.82626	$B_{30}N_{30}$ (9c)	S_{10}	−2391.08837
$B_{20}N_{20}$ (4a)	C_2	−1593.90192	$B_{30}N_{30}$ (9d)	C_{6h}	−2390.81435
$B_{20}N_{20}$ (4b)	C_{4h}	−1593.93149	$B_{32}N_{32}$ (10a)	C_1	−2550.63859
$B_{20}N_{20}$ (4c)	S_{10}	−1593.91435	$B_{32}N_{32}$ (10b)	S_8	−2550.62638
$B_{22}N_{22}$ (5a)	C_3	−1753.38576	$B_{34}N_{34}$ (11a)	C_3	−2710.11515
$B_{22}N_{22}$ (5b)	C_2	−1753.36011	$B_{34}N_{34}$ (11b)	C_2	−2710.03702
$B_{24}N_{24}$ (6a)	S_4	−1912.83071	$B_{36}N_{36}$ (12a)	T_d	−2869.57670
$B_{24}N_{24}$ (6b)	S_8	−1912.83454	$B_{36}N_{36}$ (12b)	C_{4h}	−2869.52613
$B_{24}N_{24}$ (6c)	S_{12}	−1912.29521	$B_{36}N_{36}$ (12c)	S_{12}	−2869.26770

Numbers given in the parentheses denote figure numbers

Table 2 Relative energies (kcal mol^{-1}) of the boron nitride molecules, B_xN_x at the B3LYP/cc-pvDZ level of theory

B_xN_x	Square–hexagon alternant	Octagonal tube	Capped octagonal tube	Decagonal tube	Dodecagonal tube
$B_{12}N_{12}$	0.0 (1a)	+133.8 (1b)			
$B_{16}N_{16}$	0.0 (2a)	+61.0 (2b)			
$B_{18}N_{18}$	0.0 (3a)		+8.9 (3b)		+408.4 (3c)
$B_{20}N_{20}$	0.0 (4a)	-18.6 (4b)		+139.1 (4c)	
$B_{22}N_{22}$	0.0 (5a)		+16.1 (5b)		
$B_{24}N_{24}$	0.0 (6a)	-2.4 (6b)			+336.0 (6c)
$B_{26}N_{26}$	0.0 (7a)		+13.2 (7b)		
$B_{28}N_{28}$	0.0 (8a)	+28.2 (8b)			
$B_{30}N_{30}$	0.0 (9a)		+21.3 (9b)	+54.0 (9c)	+226.0 (9d)
$B_{32}N_{32}$	0.0 (10a)	+7.7 (10b)			
$B_{34}N_{34}$	0.0 (11a)		+49.0 (11b)		
$B_{36}N_{36}$	0.0 (12a)	+31.7 (12b)			+193.9 (12c)

Numbers given in the parentheses denote figure numbers

to square–hexagon alternant over a wide range of molecule sizes. Larger tubes are not as stable, however. Tubes with a decagonal structure are less stable than octagonal tubes, and the decagonal tubes will be comparable in stability to alternants only at large sizes or perhaps not at all. The dodecagonal tubes are very unstable relative to square–hexagon alternants and octagonal tubes across the range of sizes in this study and, in all likelihood, at larger sizes as well. The general trend is toward decreasing tube stability with increasing tube diameter. Therefore, tubes based on openings larger than 12-membered rings are likely even less stable.

References

1. Jensen F (1993) Chem Phys Lett 209:417–422
2. Silaghi-Dumitrescu I, Lara-Ochoa F, Bishof P, Haiduc I (1996) J Mol Struct (Theochem) 367:47–54
3. Chopra NG, Luyken RJ, Cherrey K, Crespi VH, Cohen ML, Louie SG, Zettl A (1995) Science 269:966–967
4. Terrones M, Hsu WK, Terrones H, Zhang JP, Ramos S, Hare JP, Castillo R, Prassides K, Cheetham AK, Kroto HW, Walton DRM (1996) Chem Phys Lett 259:568–573
5. Loiseau A, Williame F, Demoncy N, Hug G, Pascard H (1996) Phys Rev Lett 76:4733–4740
6. Saito Y, Maida M (1999) J Phys Chem A 103:1291–1293
7. Martin JML, El-Yazal J, Francois JP, Gijbels R (1995) Chem Phys Lett 232:289–294
8. Martin JML, El-Yazal J, Francois JP (1996) Chem Phys Lett 248:95–101
9. Strout DL (2000) J Phys Chem A 104:3364–3366
10. Strout DL (2001) J Phys Chem A 105:261–263
11. Wu HS, Xu XH, Zhang FQ, Jiao H (2003) J Phys Chem A 107:6609–6612
12. Strout DL (2004) Chem Phys Lett 383:95–98
13. Wu HS, Jiao H (2004) Chem Phys Lett 386:369–372 (This relationship has been confirmed further: Zope RR, Baruah T, Pederson MR, Dunlap BI (2004) Chem Phys Lett 394:300–304)
14. Pokropivny VV, Skorokhod VV, Oleinik GS, Kurdyumov AV, Bartnitskaya TS, Pokropivny AV, Sisonyuk AG, Sceichenko DM (2000) J Solid State Chem 154:214–222
15. Becke AD (1993) J Chem Phys 98:5648–5652
16. Lee C, Yang W, Parr RG (1988) Phys Rev B 37:785–789
17. Dunning TH Jr (1989) J Chem Phys 90:1007–1023
18. Frisch MJ, Trucks GW, Schlegel HB, Scuseria GE, Robb MA, Cheeseman JR, Zakrzewski VG, Montgomery JA, Stratmann RE, Burant JC, Dapprich S, Millam JM, Daniels AD, Kudin KN, Strain MC, Farkas O, Tomasi J, Barone V, Cossi M, Cammi R, Mennucci B, Pomelli C, Adamo C, Clifford S, Ochterski J, Petersson GA, Ayala PY, Cui Q, Morokuma K, Malick DK, Rabuck AD, Raghavachari K, Foresman JB, Cioslowski J, Ortiz JV, Stefanov BB, Liu G, Liashenko A, Piskorz P, Komaromi I, Gomperts R, Martin R.L, Fox DJ, Keith T, Al-Laham MA, Peng CY, Nanayakkara A, Gonzalez C, Challacombe M, Gill PMW, Johnson BG, Chen W, Wong MW, Andres JL, Head-Gordon M, Replogle ES, Pople JA (1998) Gaussian 98. Gaussian Inc, Pittsburgh, PA
19. Wu HS, Cui XY, Qin XF, Jiao H (2005) J Mol Struct (Theochem) 714:153–155
20. Wu HS, Cui XY, Xu XH (2005) J Mol Struct (Theochem) 717:107–109